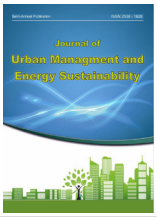
International Journal of Urban Management and Energy Sustainability (IJUMES)

Homepage: http://www.ijumes.com



CASE STUDY RESEARCH PAPER

Experimental Investigation of the Shear Strength Behavior of Two-Part Fiber-Reinforced Geopolymer Concrete Incorporating Hybrid PP/PVA Fibers

Ali Jafari[1], Reza Farokhzad[1*], Pooria Rashvand[1], Nima Amani[2]

1* *Department of Civil Engineering, Qa.C., Islamic Azad University, Qazvin, Iran*

2 *Department of Civil Engineering, Cha. C., Islamic Azad University, Chalus, Iran*

ARTICLE INFO

Article History:
Received 2026-03-01
Revised 2026-05-08
Accepted 2026-07-02

Keywords:
Geopolymer repair concrete; Hybrid fibres; interfacial bond strength; Nano-silica; Slant-shear test

ABSTRACT

The bond between existing concrete and a repair layer governs the load transfer and durability of repaired structures. Slag-based geopolymer repair materials are a lower-carbon alternative to Portland cement systems, but achieving adequate interfacial adhesion with old concrete remains a challenge. This study investigated how the nano-silica replacement level and particle size affect the interfacial bond of a slag-based geopolymer repair concrete reinforced with hybrid polypropylene and polyvinyl alcohol fibres. Ten mixtures combined NS replacement levels of 0%, 1%, 3% and 5% and nominal particle sizes of 8, 15 and 30 nm, at constant fibre contents of 0.5% PP and 0.5% PVA. Repair layers were cast on sandblasted Portland cement concrete substrates and tested at 28 days in 30° slant-shear and 90° direct-shear configurations; scanning electron microscopy and fracture surfaces were used to examine the interface. NS improved interfacial bond relative to the reference mixture, and the mixture with 3% NS of 8 nm performed best in both configurations. Increasing NS from 3% to 5% gave no consistent further gain, indicating an optimum governed by particle packing, binder reactivity and dispersion. Slant shear gave higher apparent bond resistance than direct shear owing to added normal compression, friction and interlock along the inclined interface. SEM revealed a compact repair matrix in intimate contact with the substrate, and failure shifted from predominantly interfacial separation towards mixed adhesive–cohesive failure, particularly in GPC3. Optimizing NS content and particle size can enhance the bond performance of hybrid-fibre geopolymer repair systems.

DOI: 10.22034/ijumes.2026.746882

Running Title: Shear Strength Behavior of Two-Part Fiber-Reinforced Geopolymer Concrete

NUMBER OF REFERENCES	NUMBER OF FIGURES	NUMBER OF TABLES
19	12	03

*Corresponding Author:
Email: *r.farokhzad@iau.ac.ir*
Phone: 00982833682975
ORCID: https://orcid.org/0000-0001-8505-8962

INTRODUCTION

Concrete is the most widely used construction material worldwide and plays a central role in infrastructure development. Nevertheless, the extensive use of ordinary Portland cement (OPC) in concrete production is associated with considerable environmental burdens. Cement manufacture is a major source of anthropogenic carbon dioxide emissions, largely because of the energy-intensive production process and the calcination of limestone (Prasad et al., 2023). Consequently, the use of industrial by-products and alternative aluminosilicate precursors has received growing attention as a means of developing more sustainable cementitious materials. Among these alternatives, geopolymer concrete produced through the alkaline activation of aluminosilicate materials, including ground-granulated blast-furnace slag (GGBS), has been investigated for its potential environmental and engineering benefits (Luan et al., 2021). The performance and service life of repaired concrete structures depend strongly on the integrity of the interface between the existing substrate and the repair material. Inadequate interfacial bond may lead to cracking, delamination, local loss of material, and reduced load-transfer capacity, ultimately compromising structural performance (Özdemir et al., 2025). The interface is affected by several interacting parameters, including substrate roughness and moisture condition, the properties of the repair material, binder-to-liquid ratio, curing regime, and the stress state imposed during testing. Improving the bond between old and new concrete is therefore essential for reliable rehabilitation, particularly where repaired members are exposed to repeated loading or aggressive environmental conditions. Fiber reinforcement is an established approach for controlling crack development and improving the post-cracking response of cementitious composites (Niyazuddin & Umesh, 2024). Polypropylene fibres are chemically stable in highly alkaline environments, exhibit low water absorption, and can restrain the initiation and propagation of microcracks. Their distribution throughout the matrix can improve deformation capacity and energy absorption (Trabacchin et al., 2022). PVA fibres, in contrast, generally develop stronger interfacial interaction with cementitious matrices because of their surface characteristics. This interaction can contribute to tensile stress transfer and crack bridging. The combined use of PP and PVA fibres may therefore provide complementary crack-control mechanisms, although the effectiveness of hybrid reinforcement depends on fibre geometry, dosage, dispersion, and matrix characteristics. In addition to fiber reinforcement, nano-scale additives can modify the pore structure and reaction products of geopolymer binders. Nano-silica has a high specific surface area and can act as a fine filler and reactive silica source. When suitably dispersed, it may promote matrix densification, modify the development of aluminosilicate and calcium-containing binding gels, and reduce the size and connectivity of pores (Ahmed et al., 2021). These effects are potentially beneficial to interfacial bond because a denser repair matrix may improve contact with the roughened substrate and reduce local stress concentrations. However, excessive nano-silica may increase water demand, impair workability, or promote particle agglomeration. Accordingly, both dosage and particle size require consideration (Meskhi et al., 2023).

Recent studies have examined the bond behaviour of geopolymer concrete and the influence of reinforcement, curing, and mixture composition. Research using pull-out tests has shown that bond-slip response is affected by parameters such as embedment length and the characteristics of the contact surface (Bayrak et al., 2024; Li et al., 2024). Other experimental and numerical investigations have further highlighted the importance of representing interfacial behaviour when assessing geopolymer-based structural systems (Hai et al., 2024; Romanazzi et al., 2025). Studies on nano-silica-modified geopolymer binders have reported that moderate additions can improve matrix compactness

and mechanical performance, whereas excessive additions may be counterproductive because of agglomeration and reduced workability (Cui et al., 2023).

Fibre-reinforced geopolymer composites have also been reported to exhibit improved crack control and residual mechanical performance. The surface interaction of PVA fibres with the binder can contribute to stress transfer, while PP fibres can provide distributed crack restraint. The combination of different fibre types may thus be useful where both microcrack control and post-cracking resistance are required (Li et al., 2025; Skane et al., 2025; Yuan et al., 2025; Zarzuela et al., 2024). In parallel, the thermal and moisture-related properties of geopolymers have been shown to depend on their chemical composition and pore structure (Liu & Ju, 2024). These findings indicate that geopolymer performance is governed by coupled chemical, microstructural, and mechanical mechanisms. Despite this progress, the interfacial bond behaviour of fibre-reinforced, nano-silica-modified geopolymer repair concrete remains insufficiently characterized, particularly when the effects of nano-silica particle size and inclined versus direct shear configurations are considered together. The present study addresses this issue by examining a slag-based geopolymer repair material modified with nano-silica at replacement levels of 1%, 3%, and 5%, using particle sizes of 8, 15, and 30 nm. All mixtures contain fixed dosages of 0.5% PP fibres and 0.5% PVA fibres to investigate their combined contribution. The repair system is evaluated against an existing OPC concrete substrate using 30° and 90° interfacial shear configurations, supported by SEM observations and fracture-surface assessment. The main objective is to clarify how nano-silica characteristics and hybrid fibre reinforcement influence interfacial resistance and the associated failure mechanisms. Figure 1 presents the schematic overview of the research background, material modification strategies, and experimental framework for evaluating the interfacial bond behavior of nano-silica-modified hybrid fibre-reinforced geopolymer repair concrete. (Fig. 1)

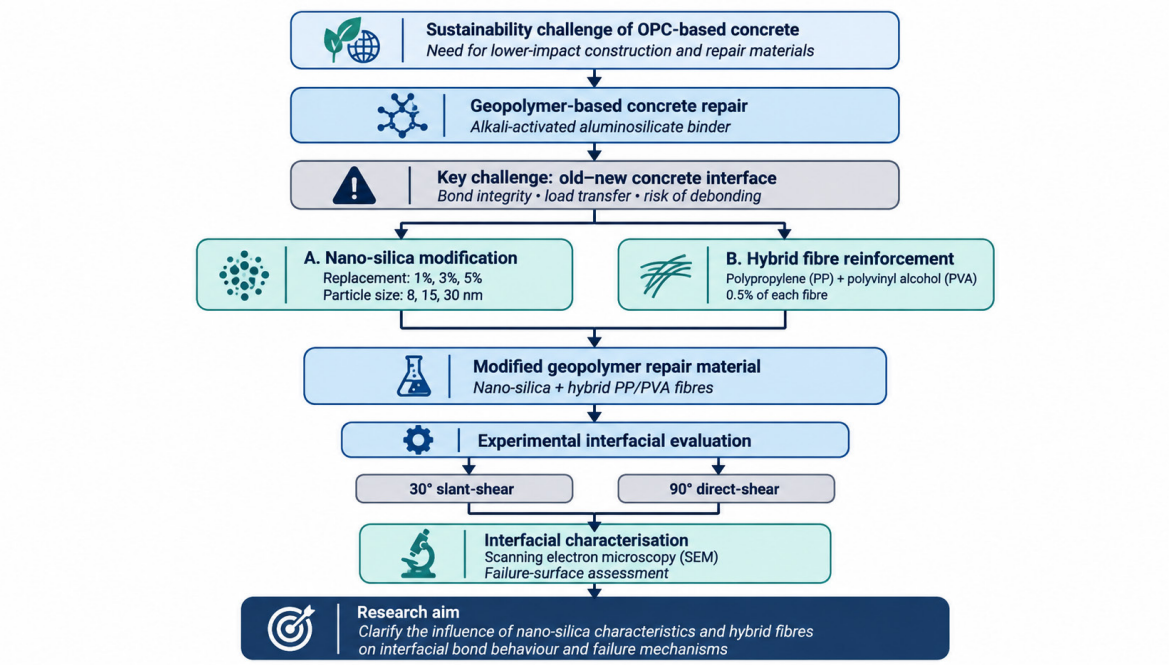


Figure 1: Schematic overview of the research background, material modification strategies, and experimental framework

MATERIALS AND METHODS

Constituent materials

The materials used to produce the geopolymer repair concrete included an aluminosilicate precursor, alkaline activator solutions, natural fine and coarse aggregates, nano-silica, and PP and PVA fibres. The alkaline activator consisted of sodium hydroxide (NaOH) and sodium silicate (Na_2SiO_3). The sodium silicate solution was supplied in gel form and contained 54.1% water, 32.5% SiO_2, and 13.4% Na_2O. The NaOH solution was prepared at a concentration of 12 mol/L using pellets with a stated purity of 95%. The NaOH pellets were dissolved in distilled water at least 24 h before mixing to allow the exothermic dissolution process to subside and the solution to return to ambient temperature. The SiO_2/Na_2O ratio adopted for the alkaline activator was 1.5. Natural sand and gravel obtained from the Amol dolomitic aggregate sources and river deposits, respectively, were used. Nano-silica was incorporated as a partial replacement for the precursor at three levels (1%, 3%, and 5%) and with nominal particle sizes of 8, 15, and 30 nm. The nano-silica, with a reported purity of 99.5%, was obtained from US Research Nano-Materials Inc. (Houston, USA). The chemical compositions of the precursor and nano-silica are summarized in Table 1. The nano-silica used in this study is shown in (Fig. 2 and Tab. 1)

Table 1: Chemical composition of the precursor and nano-silica.

Component (%)	GGBS	Nano-silica
SiO2	32.57	≥ 99
Al2O3	1.26	-
Fe2O3	3.3	-
CaO	34.07	-
MgO	0.89	-
SO3	0.5	-
Na2O	1.12	-
K2O	0.56	-
Loss of ignition	2.28	0.2

The aggregate grading is presented in Figure 3. The reported water absorption values for the fine and coarse aggregates were approximately 2.8% and 2.1%, respectively, while their specific gravity values were reported as 2.565 and 2.580. Aggregate characterization was conducted with reference to ASTM C33/C33M (ASTM International, 2024). (Fig. 2 and 3)

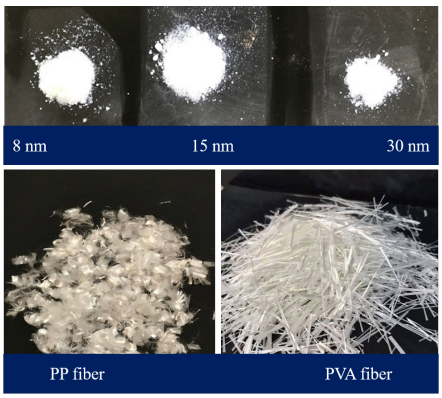


Figure 2: Nano-silica particles used in this study.

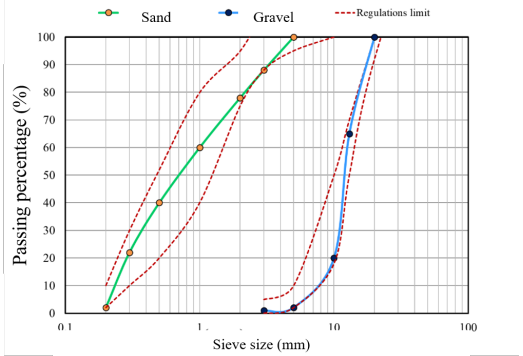


Figure 3: Particle-size distribution of the aggregates (green: sand; blue: gravel).

Hybrid fiber reinforcement was provided by PP and PVA fibres at a fixed dosage of 0.5% for each fibre type in all modified mixtures. The PP fibres were 6 mm long and had a density of 0.93 g/cm³; they were supplied by Mana Fiber, Delijan, Iran. The PVA fibres had a diameter of 10 µm and a length of 12 mm and were supplied by FaraTav, Iran.

Mixture proportions and specimen configuration

Ten geopolymer repair mixtures containing slag, nano-silica, and hybrid PP/PVA fibres were designed to evaluate the bond between the existing concrete substrate and the repair layer. The substrate concrete was produced using Type II Portland cement and had a nominal strength class of 20 MPa. The alkali-to-binder ratio adopted in the mixtures was 0.35. Before application of the repair material, the substrate surface was roughened by sandblasting. The substrate was brought to a saturated-surface-dry (SSD) condition before casting the repair layer. The repaired specimens were evaluated after 28 days. Two interfacial configurations were investigated: a direct-shear configuration with the interface oriented at 90° and an inclined configuration at 30°. Loading was applied to induce shear transfer across the interface. The specimen dimensions were 75 × 75 × 280 mm. A groove was formed in the middle region of the mould to create the required inclined interface. The old concrete surface was prepared in two conditions: grooved, and grooved followed by wire brushing. These surface conditions were used to assess the contribution of surface texture to interfacial performance. (Fig. 4 and 5)

A grinder was used to create grooves in two oblique directions on the damaged substrate surface. ImageJ analysis was used to compare the surface texture produced by grooving alone with that produced by combined grooving and brushing. The image-based assessment indicated that the combined treatment generated secondary fine-scale irregularities on the primary grooves and a more uniformly distributed surface texture. In principle, this can increase the effective contact area and provide additional locations for mechanical interlock. These observations are qualitative unless supported by a calibrated roughness parameter; therefore, the

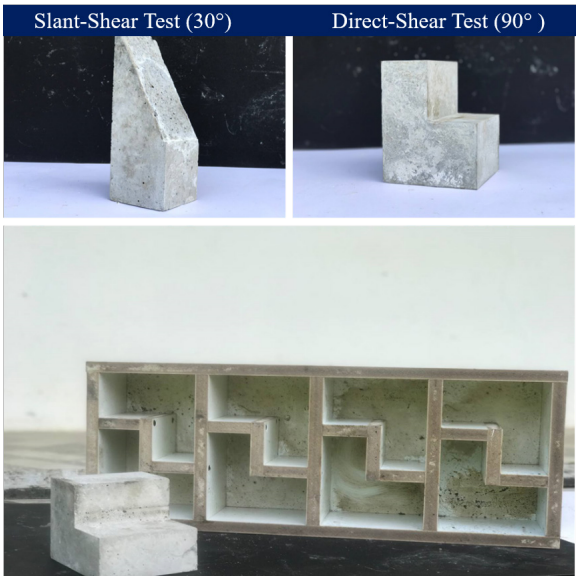


Figure 4: Specimen preparation and composite specimens with Portland-cement concrete as the existing substrate.



Figure 5: Grooving of the substrate surface.

image analysis should not be interpreted as a direct measurement of interfacial shear capacity. (Tab. 2)

Table 2: Mixture proportions of the geopolymer repair mixtures.

Sample ID	Sand (kg/m3)	Gravel (kg/m3)	Water (kg/m3)	GGBS (kg/m3)	NS (kg/m3)	NS (%)	PP (%)	PVA (%)	NS (nm)
GPC0	500	1036	121	295	0	0	0.5	0.5	0
GPC1-D8	500	1036	121	292	2.9	1	0.5	0.5	8
GPC1-D15	500	1036	121	292	2.9	1	0.5	0.5	15
GPC1-D30	500	1036	121	292	2.9	1	0.5	0.5	30
GPC3-D8	500	1036	121	286	8.8	3	0.5	0.5	8
GPC3-D15	500	1036	121	286	8.8	3	0.5	0.5	15
GPC3-D30	500	1036	121	286	8.8	3	0.5	0.5	30
GPC5-D8	500	1036	121	280	14.7	5	0.5	0.5	8
GPC5-D15	500	1036	121	280	14.7	5	0.5	0.5	15
GPC5-D30	500	1036	121	280	14.7	5	0.5	0.5	30

Because dissolution of NaOH in water is highly exothermic, the alkaline solution was prepared one day before mixing and allowed to cool to ambient temperature.

Mixing, casting, and curing

The first half of each composite specimen was cast using conventional Portland-cement concrete. After 28 days of water curing, this portion was used as the existing substrate. Its contact surface was roughened by sandblasting and prepared according to the designated surface condition. The geopolymer repair mixture was then placed against the prepared substrate. The geopolymer mixtures were produced in a 50-L pan mixer. The aggregates were first introduced and mixed to obtain a uniform granular blend. The precursor and nano-silica were then added and mixed with the aggregates. PP and PVA fibres were gradually introduced separately to minimise fibre balling and promote dispersion. Finally, the alkaline activator, comprising sodium hydroxide and sodium silicate solutions, was added to the dry constituents, and mixing continued for approximately 2 min. After mixing and fresh-state inspection, the material was placed in pre-oiled molds. The Portland-cement substrate specimens were water-cured. The geopolymer repair portions were heat-cured in an oven at 60 °C for 24 h and subsequently stored at ambient laboratory conditions until testing. The bond response was assessed at 28 days. Figure 6 illustrates the curing regimes adopted for the substrate and repair materials. (Fig. 6)



Figure 6: Curing conditions for the substrate and geopolymer repair portions.

FINDINGS AND DISCUSSION

The bond between existing concrete and a repair layer governs the extent to which the two materials act compositely under load. Insufficient interfacial resistance can cause premature cracking or delamination, reducing load transfer and potentially accelerating deterioration. The bond response is influenced by substrate roughness,

moisture condition, repair-material properties, fibre reinforcement, curing, and the stress distribution imposed by the test configuration. In the present study, the influence of nano-silica modification and hybrid fibre reinforcement was considered together with the orientation of the interface.

Bond behavior under slant shear at 30°

Figure 7 presents the bond-test results for the interface between the existing cement-based substrate and the geopolymer repair layer under the 30° inclined configuration. The test procedure was adapted from ASTM D4541-22 (ASTM International, 2022). (Fig. 7)

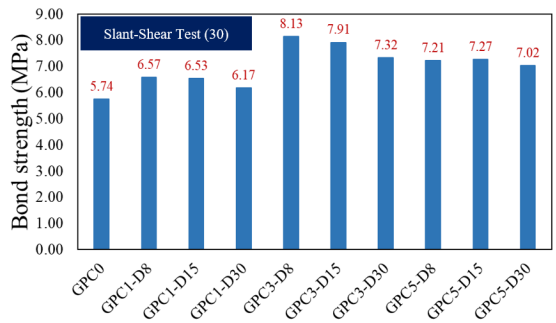


Figure 7: Interfacial bond response under the 30° slant-shear configuration.

The results show that the nano-silica-modified mixtures generally exhibited improved interfacial performance compared with the reference mixture. Among the investigated combinations, the mixture containing 3% nano-silica with a nominal particle size of 8 nm (GPC3-D8) provided the most favourable response. A plausible explanation is that a moderate nano-silica dosage can improve particle packing and promote the development of a denser binding matrix. In a slag-containing alkali-activated system, the reaction products may include calcium-(alumino)-silicate-hydrate-type gels (C-(A)-S-H) together with sodium aluminosilicate hydrate (N-A-S-H)-type products, depending on precursor chemistry and activator composition. The inclined configuration combines interfacial shear with a compressive component that can increase contact pressure and frictional resistance along the interface. Consequently, the measured resistance may include contributions from adhesion, aggregate or surface interlock, and friction under compression. The roughened substrate can further promote mechanical engagement between the repair matrix and surface irregularities. The hybrid PP/PVA fibres may restrain crack opening and distribute local stresses in the repair layer; however, their contribution to interfacial resistance should be interpreted as indirect unless fibre bridging across the interface is directly observed. The superior response of GPC3-D8 is consistent with an optimum balance between nano-scale filling and binder reactivity. At lower replacement levels, the amount of nano-silica may be insufficient to achieve the maximum densification effect. At higher levels, particle agglomeration and increased liquid demand may offset the benefits of additional silica. This interpretation is consistent with the non-monotonic response observed across the investigated replacement levels, although direct confirmation of agglomeration would require additional microstructural or dispersion measurements. (Fig. 8)



Figure 8: Moulding arrangement used for the slant-shear specimens.

Bond behaviour under direct shear at 90°

The direct-shear configuration was used to evaluate the interface at 90°. In this arrangement, the applied force was intended to transfer shear across the interface, and the specimens were tested using a universal testing machine (UTM), as shown in Figure 9. (Fig. 9)



Figure 9: Universal testing machine used for interfacial bond evaluation.

Figure 10 presents the results of the 90° direct-shear tests. The measured bond resistance was lower than that obtained from the 30° inclined configuration. This difference can be attributed, at least in part, to the different stress states generated by the two configurations. In the 90° arrangement, resistance is more strongly governed by the interface's adhesion and surface interlock, whereas the inclined configuration may introduce a compressive component that increases frictional resistance and suppresses relative sliding. Accordingly, the results from the two configurations should be regarded as configuration-dependent apparent bond strengths rather than directly interchangeable material properties. (Fig. 10)

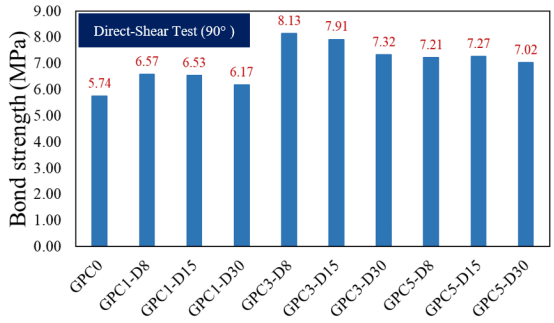


Figure 10: Direct shear test response under the 90° direct-shear configuration.

Across the investigated mixtures, nano-silica improved the bond response, with the 3% dosage and 8 nm particle size producing the best overall performance. The 1% nano-silica mixtures showed a more limited improvement, while the 5% mixtures did not consistently outperform the 3% mixtures. This trend suggests that nano-silica dosage must be optimised rather than increased continuously. The combined PP/PVA fibres may have contributed to crack restraint and energy absorption within the repair material. PP fibres can provide distributed microcrack control, whereas PVA fibres can develop stronger interaction with the surrounding binder. The highest bond response was recorded for GPC3-D8, while the reference mixture without nano-silica showed the least favorable performance. (Tab. 3)

Table 3: Comparative assessment of the interfacial performance of the investigated mixtures.

Sample ID	NS (%)	NS (nm)	Continuity function
GPC0 (Reference sample)	0	0	Minimal; superficial failure at the interface
GPC1-D8	1	8	Relative improvement; increased adhesion, limited density
GPC1-D15	1	15	Moderate improvement; moderate microstructural density

GPC1-D30	1	30	Low effect; tendency for particles to aggregate
GPC3-D8	3	8	Maximum strength; dense microstructure, failure within the new concrete
GPC3-D15	3	15	Significant improvement; appropriate density and continuity
GPC3-D30	3	30	Moderate; relative accumulation of particles hinders full performance.
GPC5-D8	5	8	Improvement, but less than 3%; reduced efficiency due to excessive density.
GPC5-D15	5	15	Limited improvement; weakness resulting from greater particle aggregation
GPC5-D30	5	30	Poorer performance; reduced efficiency and density

Mechanical interlock at the old–new concrete interface

The stress-transfer mechanism at a repair interface depends strongly on interface orientation and the resulting combination of normal and shear stresses. Under the 90° configuration, the applied load is transferred predominantly as shear along the interface, making the response particularly sensitive to adhesion and surface roughness. Under the 30° configuration, the inclined geometry can generate a compressive component normal to the interface. This component may increase contact pressure and friction, thereby delaying sliding and promoting mechanical interlock. The higher resistance measured in the inclined configuration is therefore consistent with the combined action of shear transfer and compression-induced friction. For GPC3-D8, the improvement may be associated with both matrix refinement and mechanical engagement with the roughened substrate. Nano-silica can fill fine voids and, when sufficiently dispersed, contribute reactive silica to the alkali-activation process. The resulting refinement of the repair matrix may improve its ability to conform to surface irregularities. Nevertheless, the precise chemical phases and the degree of penetration into the substrate cannot be established from bond tests alone; they should be interpreted in conjunction with SEM/EDS, XRD, or other appropriate characterisation.

Microstructural characteristics of the repaired interface

The interfacial microstructure was examined by scanning electron microscopy at a magnification of 500×. Figure 11 shows the contact region between the existing concrete and the nano-silica-containing geopolymer repair material. The lower region, corresponding to the old concrete, appears comparatively heterogeneous and porous, with visible irregularities and pores. Such surface features can provide anchorage points for the repair material. The upper region, corresponding to the geopolymer repair layer, appears more compact and relatively uniform in the presented micrograph. A gradual transition between the two regions is visible in the interfacial area. The observed contact suggests that the fresh repair material occupied some of the surface irregularities of the substrate, potentially contributing to mechanical interlock. The denser appearance of the repair matrix is consistent with a filler effect of fine nano-silica and the formation of alkali-activation products. In slag-containing systems, calcium-bearing reaction products may coexist with sodium aluminosilicate gels. However, SEM morphology alone cannot unambiguously identify N-A-S-H, C-(A)-S-H, or calcium carbonate; phase identification requires complementary chemical or crystallographic evidence. The following microstructural features may be considered when interpreting the image: (i) reaction-product gels, potentially comprising N-A-S-H and calcium-(alumino)-silicate hydrate-type phases; (ii) pore filling and local densification in the repair matrix; (iii) possible carbonation products where exposure to atmospheric CO_2 has occurred; and (iv) partially reacted precursor or silica-rich particles embedded in the gel matrix. These interpretations should be treated as plausible mechanisms rather than definitive phase identifications unless supported by EDS or XRD results. (Fig. 11)

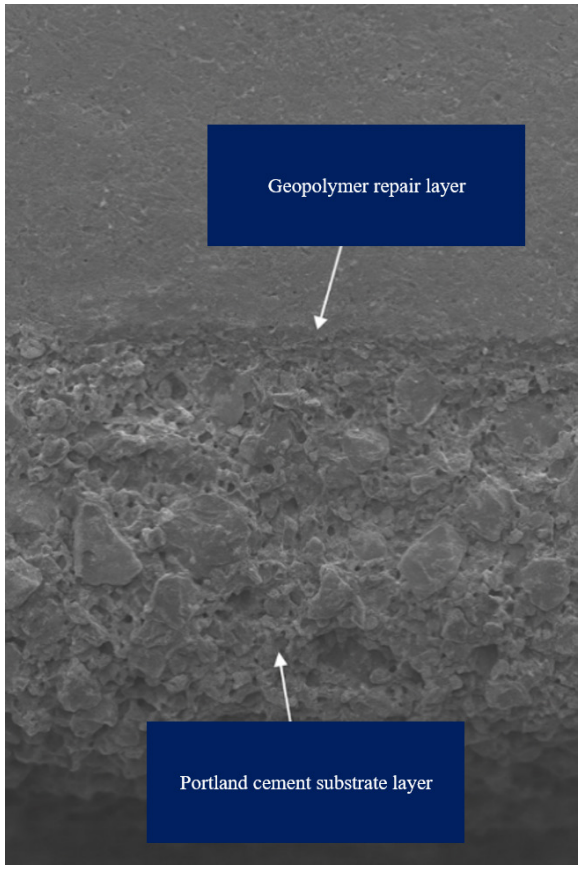


Figure 11: SEM micrograph of the interface between the existing concrete and the geopolymer repair layer.

Failure-mode analysis

The failure surfaces were examined to identify whether fracture occurred predominantly along the interface or within one of the constituent materials. In general, a predominantly interfacial (adhesive) failure indicates that the interface is weaker than the adjacent matrices, whereas cohesive failure indicates that fracture has propagated through the repair material or substrate. Mixed failure involves both mechanisms and may indicate that the interfacial resistance has approached the strength of one or both adjoining materials. For the GPC1 mixture containing 1% nano-silica, separation was observed largely along the interface between the conventional concrete and the geopolymer repair layer. The relatively smooth fracture region and limited penetration of the crack into the adjoining materials are consistent with a substantial adhesive component. Nevertheless, portions of geopolymer material remained attached to the substrate, and the crack locally extended into the repair layer. Thus, the observed failure is more accurately described as mixed adhesive–cohesive rather than exclusively adhesive or exclusively cohesive. For GPC3, the crack initiated near the interface but propagated into the geopolymer repair layer in some regions. The presence of repair material remaining on the substrate indicates that failure was not confined entirely to the interface. This observation is consistent with an improved interfacial bond and a mixed adhesive-cohesive failure mode. The denser repair matrix associated with the 3% nano-silica mixture may have contributed to the improved stress transfer, although the precise mechanism cannot be isolated from fracture images alone. The GPC5 specimen containing 5% nano-silica also exhibited evidence of mixed failure. Crack propagation was not restricted to a clean separation along the interface; instead, portions of the fracture path extended into the repair layer or interfacial transition region. The failure can therefore be classified as mixed, with a relatively more pronounced adhesive component than that observed for the best-performing GPC3 mixture. This is consistent with the bond-test trend in which increasing nano-silica content beyond the optimum did not provide a further improvement. (Fig. 12)

RESULTS AND CONCLUSION

This study experimentally investigated the interfacial bond behaviour of a slag-based geopolymer repair concrete modified with nano-silica and hybrid PP/PVA fibres. The effects of nano-silica replacement level and particle size were evaluated using 30° slant-shear and 90° direct-shear configurations, together with SEM observations and fracture-surface assessment. The principal conclusions are as follows:

•Among the mixtures investigated, the combi-

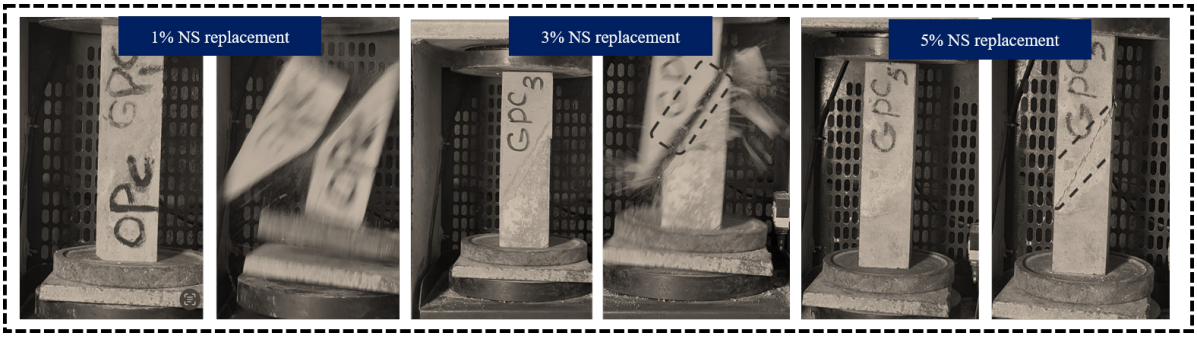


Figure 12: Failure surface of the GPC5 specimen containing 5% nano-silica.

nation of 3% nano-silica with a nominal particle size of 8 nm (GPC3-D8), together with 0.5% PP and 0.5% PVA fibres, produced the most favourable interfacial bond performance. This behaviour is plausibly associated with improved particle packing, matrix refinement, and enhanced contact with the roughened substrate.

•The response did not increase monotonically with nano-silica content. The 1% mixtures showed a more limited improvement, whereas increasing the replacement level to 5% did not produce a further gain. This indicates the importance of optimising nano-silica dosage and dispersion.

•The 30° slant-shear configuration produced higher apparent bond resistance than the 90° direct-shear configuration. The difference is consistent with the additional compressive component and frictional resistance that can develop in the inclined configuration. Results from these configurations should therefore be interpreted in light of their distinct stress states.

•The combined PP/PVA fibre system may have contributed to microcrack restraint and energy dissipation within the repair matrix. The complementary roles of PP and PVA fibres provide a plausible explanation for improved crack control, although the present test programme does not isolate the individual contribution of each fibre type.

•SEM observations showed a relatively compact repair matrix and intimate contact with irregularities in the existing concrete. These features are consistent with improved mechanical interlock and interfacial performance. Definitive identification of reaction products, however, requires complementary chemical or crystallographic analyses.

•Fracture-surface observations indicated a transition from predominantly interfacial separation in the lower-performing mixture toward mixed adhesive–cohesive failure in nano-silica-modified mixtures, particularly GPC3. This shift is consistent with an improvement in interfacial resistance.

The findings suggest that nano-silica-modified, hybrid-fibre geopolymer concrete has potential as a repair material for existing concrete structures. Further work should quantify interfacial roughness, report replicate numbers and statistical dispersion, clarify the exact stress and bond-strength calculations for each test geometry, and evaluate repaired structural members under realistic static, cyclic, and environmental loading. Numerical and machine-learning models may also be developed once a sufficiently large and internally consistent experimental database is available.

REFERENCES

Ahmed, H. U., Mohammed, A. A., Rafiq, S., Mohammed, A. S., Mosavi, A., Sor, N. H., et al. (2021). Compressive strength of sustainable geopolymer concrete composites: A state-of-the-art review. Sustainability, 13(24), 13502. https://doi.org/10.3390/su132413502

ASTM International. (2022). Standard test method for pull-off strength of coatings using portable adhesion testers (ASTM D4541-22). https://doi.

org/10.1520/D4541-22

ASTM International. (2024). Standard specification for concrete aggregates (ASTM C33/C33M-24a). https://doi.org/10.1520/C0033_C0033M-24A

Bayrak, B., Akarsu, O., Kılıç, M., Alcan, H. G., Çelebi, Ö., Kaplan, G., et al. (2024). Experimental study of bond behavior of geopolymer concrete under different curing conditions using a pull-out test. Construction and Building Materials, 439, 137357. https://doi.org/10.1016/j.conbuildmat.2024.137357

Cui, Y., Ai, W., Tekle, B. H., Liu, M., Qu, S., & Zhang, P. (2023). State-of-the-art review on the production and bond behaviour of geopolymer concrete. Discover Civil Engineering. https://doi.org/10.1007/s44242-023-00027-1

Hai, R., Ma, Z., Chen, X., Cao, Y., Zhang, J., & Hui, C. (2024). Experimental and numerical investigations on the bond-slip behavior of the interface between geopolymer concrete and steel tube. Scientific Reports, 14, Article 79964. https://doi.org/10.1038/s41598-024-79964-1

Li, J., Yang, L., Xie, H., Gao, J., Zhang, F., & Chen, S. (2025). Bond behavior between geopolymer recycled brick aggregate concrete and reinforcement: Pull-out test results. Construction and Building Materials. [Volume, article number and DOI to be completed by the authors]

Li, Z., Tan, J., Ouyang, J., Yu, Y., Li, S., Lin, T., et al. (2024). Experimental investigation of the bond performance at the interface between engineered geopolymer composites and existing concrete. Buildings, 14(6), 1819. https://doi.org/10.3390/buildings14061819

Liu, W., & Ju, S. (2024). Tunable thermal conductivity of sustainable geopolymers by Si/Al ratio and moisture content: Insights from atomistic simulations [Preprint]. arXiv. https://arxiv.org/abs/2401.11522

Luan, C., Wang, Q., Yang, F., Zhang, K., Utashev, N., Dai, J., et al. (2021). Practical prediction models of tensile strength and reinforcement-concrete bond strength of low-calcium fly ash geopolymer concrete. Polymers, 13(6), 875. https://doi.org/10.3390/polym13060875

Meskhi, B., Beskopylny, A. N., Stel'makh, S. A., Shcherban', E. M., Mailyan, L. R., Shilov, A. A., et al. (2023). Analytical review of geopolymer concrete: Retrospective and current issues. Materials, 16(10), 3792. https://doi.org/10.3390/ma16103792

Niyazuddin, & Umesh, B. (2024). Experimental investigation on bond behaviour of the GFRP bars with normal and high strength geopolymer concrete. Construction and Building Materials, 429, 136395. https://doi.org/10.1016/j.conbuildmat.2024.136395

Özdemir, M. H. S., Bayrak, B., & Aydın, A. C. (2025). Bond performance of geopolymer concrete with basalt/glass fiber under elevated temperature. Engineering Structures, 324, 119368. https://doi.org/10.1016/j.engstruct.2024.119368

Prasad, B. V., Anand, N., Kanagaraj, B., Kiran, T., Lublóy, É., Naser, M. Z., Arumairaj, P. D., & Andrushia, D. (2023). Investigation on residual bond strength and microstructure characteristics of fiber-reinforced geopolymer concrete at elevated temperature. Case Studies in Construction Materials, 19, e02526. https://doi.org/10.1016/j.cscm.2023.e02526

Romanazzi, V., Leone, M., & Aiello, M. A. (2025). Bond performance of geopolymer concrete with steel and FRP reinforcements. Journal of Composites Science, 9(6), 303. https://doi.org/10.3390/jcs9060303

Skane, R., Schneider, P. A., Rickard, W. D. A., Jones, F., van Riessen, A., Jamieson, E., et al. (2025). Predicting the stability of geopolymer activator solutions for optimized synthesis through thermodynamic modelling [Preprint]. arXiv. https://arxiv.org/abs/2503.12942

Trabacchin, G., Sebastian, W., & Zhang, M. (2022). Experimental and analytical study of bond between basalt FRP bars and geopolymer concrete. Construction and Building Materials, 315, 125461. https://doi.org/10.1016/j.conbuildmat.2021.125461

Yuan, J., Xiao, J., & Huang, D. (2025). Experimental research on bond behavior of high-strength reinforcement in unconfined fly ash-based geopolymer concrete [Preprint]. SSRN. https://doi.org/10.2139/ssrn.5217139

Zarzuela, R., Luna, M. L., Carrascosa, L. M., Yeste, M. P., Garcia-Lodeiro, I., Blanco-Varela, M. T., et al. (2024). Producing C-S-H gel by reaction between silica oligomers and portlandite: A promising approach to repair cementitious materials [Preprint]. arXiv. https://arxiv.org/

abs/2401.14118

COPYRIGHTS
©2023 The author(s). This is an open access article distributed under the terms of the Creative Commons Attribution (CC BY 4.0), which permits unrestricted use, distribution, and reproduction in any medium, as long as the original authors and source are cited. No permission is required from the authors or the publishers.

HOW TO CITE THIS ARTICLE
Jafari, A., Farokhzad, R. & Rashvand, P. (2026). Experimental Investigation of the Shear Strength Behavior of Two-Part Fiber-Reinforced Geopolymer Concrete Incorporating Hybrid PP/PVA Fibers. (e746882). International Journal of Urban Management and Energy Sustainability, 7(2), e746882
DOI: 10.22034/ijumes.2026.746882